

Theory of nonlinear optical spectroscopy of electron spin coherence in quantum dots

Ren-Bao Liu,¹ S. E. Economou,² L. J. Sham,² and D. G. Steel³¹*Department of Physics, The Chinese University of Hong Kong, Shatin, New Territories, Hong Kong, China*²*Department of Physics, University of California San Diego, La Jolla, California 92093-0319, USA*³*The H. M. Randall Laboratory of Physics, University of Michigan, Ann Arbor, Michigan 48109, USA*

(Received 3 October 2006; published 26 February 2007)

We study in theory the generation and detection of electron spin coherence in nonlinear optical spectroscopy of semiconductor quantum dots doped with single electrons. In third-order differential transmission spectra, the inverse width of the ultranarrow peak at degenerate pump and probe frequencies gives the longitudinal spin relaxation time (T_1), and that of the Stokes and anti-Stokes spin resonances gives the spin dephasing time including the inhomogeneous broadening (T_2^*). The transverse spin relaxation time excluding the inhomogeneous broadening effect (T_2) can be measured by the inverse width of ultranarrow hole-burning resonances in fifth-order differential transmission spectra.

DOI: [10.1103/PhysRevB.75.085322](https://doi.org/10.1103/PhysRevB.75.085322)

PACS number(s): 78.67.Hc, 76.70.Hb, 42.65.An

I. INTRODUCTION

Electron spin coherence in semiconductor quantum dots (QDs) is a quantum effect to be exploited in emerging technologies such as spin-based electronics (spintronics) and quantum computation.¹ The electron spin decoherence is a key issue for practical application of the electron spin freedom and is also of fundamental interest in mesoscopic physics and in quantum physics. The electron spin decoherence in QDs, however, is yet poorly characterized. By convention, the spin decoherence is classified into the longitudinal and the transverse parts, which correspond to the spin population flip and the Zeeman energy fluctuation processes and are usually characterized by the longitudinal relaxation time T_1 and the transverse relaxation time T_2 , respectively. Most current experiments are carried out on ensembles of spins, composed of either many similar QDs (Refs. 2–5) or many repetitions of (approximately) identical measurements on a single QD.^{6–14} The ensemble measurements are subjected to the inhomogeneous broadening of the Zeeman energy, which results from the fluctuation of the QD size, shape, and compound composition (and in turn the electron g -factor) and from the random distribution of the local Overhauser field (due to the hyperfine interaction with nuclear spins in thermal states). The inhomogeneous broadening leads to a dephasing time T_2^* .^{15–17} The three time scales characterizing the electron spin decoherence can differ by orders of magnitude usually in the order of $T_1 \gg T_2 \gg T_2^*$. For example, in a typical GaAs QD at a low temperature (≤ 4 K) and under a moderate to strong magnetic field (0.1–10 T), the longitudinal relaxation time T_1 can be in the order of milliseconds,^{6–11,18} the transverse relaxation time T_2 is up to several microseconds,^{5,12,14} and the dephasing time T_2^* can be as short as a few nanoseconds.^{3,5,12,13}

The issue is how to measure the characteristic times of electron spin decoherence in QDs. There have been many experiments both in optics^{4,9–11,18} and in transport,^{6–8} which establish the longitudinal spin relaxation time T_1 in QDs of different materials. The dephasing time T_2^* has also been measured for QD ensembles,^{2,3,5,12,13} giving a lower bound of T_2 . Spin echo in microwave electron spin resonance (ESR)

experiments is a conventional approach to measuring the transverse spin relaxation time T_2 excluding the inhomogeneous broadening,^{19–21} which, however, is less feasible for III-V compound quantum dots due to the fast time scales in such systems ($T_2 \lesssim 10^{-6}$ s and $T_2^* \lesssim 10^{-9}$ s). Indeed, the remarkable spin echo experiments in coupled QDs done by Petta *et al.* are performed with rather long dc voltage pulses instead of instantaneous microwave pulses.¹² Alternatively, picosecond optical pulses may be used to manipulate electron spins via Raman processes²² and realize the spin echo, which, however, still need to overcome the difficulty of stabilizing and synchronizing picosecond pulses in microsecond time spans. A recent experiment by Grelich *et al.* also shows that the inhomogeneous broadening effect can be filtered out from the spin coherence mode locked by a periodic train of laser pulses.⁵

In this paper, we will study the frequency-domain nonlinear optical spectroscopy as another approach to measuring the electron spin decoherence times. Particularly, the transverse relaxation rate T_2^{-1} is correlated to the width of ultranarrow hole-burning peaks in fifth-order differential transmission (DT) spectra. This hole-burning measurement of the spin relaxation time is analogous to the exploration of slow relaxation of optical coherence in atomic systems by the third-order hole-burning spectroscopy.²³ Here, the fifth-order nonlinearity is needed because the creation of spin coherence by Raman processes involves at least two orders of optical field and hole-burning two more. The state-of-the-art spectroscopy already has the ultrahigh resolution (much better than megahertz-resolution) to resolve the slow spin decoherence in microsecond or even millisecond time scales.^{24–26}

The organization of this paper is as follow. After this introductory section, Sec. II describes the model for the QD system and the master-equation approach to calculating the nonlinear optical susceptibility. Section III presents the results and discussion. Section IV concludes this paper. The solution of the master equation in the frequency domain is presented in the Appendix.

II. MODEL AND THEORY

The system to be studied is a semiconductor QD doped with a single electron. The geometry of the QD under an

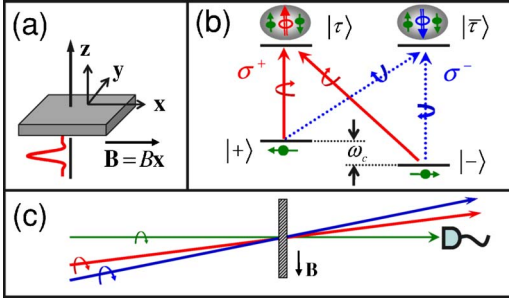


FIG. 1. (Color online) Schematics of (a) the quantum dot, (b) the selection rules for optical transitions, and (c) the optical detection geometry.

external magnetic field and optical excitation is shown in Figs. 1(a) and 1(c). The QD is assumed to be a shape with small thickness in the growth direction and relatively large radius in the lateral directions, as in the usual cases of fluctuation GaAs QDs.^{3,10} To enable the generation and manipulation of the electron spin coherence through Raman processes, a magnetic field is applied along a lateral direction (x axis). The propagation directions of the pump and probe laser beams are close to the growth direction (z axis). The two electron spin states $|\pm\rangle$ are split by the magnetic field with Zeeman energy ω_0 . The strong confinement along the z axis induces a large splitting between the heavy hole and the light hole states, thus the relevant exciton states are the ground trion states $|\tau\rangle$ and $|\bar{\tau}\rangle$, which consist of two electrons (including the doped one and one created by optical excitation) in the singlet spin state and one heavy hole in the spin states $|+3/2\rangle$ and $|-3/2\rangle$ (quantized along the z axis with nearly zero Zeeman splitting), respectively. Similarly, we can also neglect the excitation of higher-lying trions, biexciton, and multiexciton states since the energy of adding an exciton in each case is well separated from energy of the lowest trion states. The selection rules for the optical transitions are determined by the (approximate) conservation of the angular momentum along the growth direction so that a circularly polarized light with polarization σ^+ or σ^- connects the two electron spin states to the trion state $|\tau\rangle$ or $|\bar{\tau}\rangle$, respectively [see Fig. 1(b)]. The relaxation processes in the system are parametrized by the exciton recombination rate Γ_1 , the exciton dephasing rate Γ_2 , the longitudinal spin relaxation time T_1 , and the transverse spin relaxation time T_2 . The inhomogeneous broadening leads to a random component ϵ to the Zeeman splitting: $\omega_c = \omega_0 + \epsilon$, which is assumed to be a Gaussian distribution $g(\epsilon) = e^{-\epsilon^2/(2\gamma^*)}/(\sqrt{2\pi}\gamma^*)$. The spin dephasing time including the inhomogeneous broadening $T_2^* \equiv 1/\gamma^* \ll T_2$, unless it is artificially set to be $T_2^* = T_2$ (by setting $\gamma_2^* = 0$). The hole spin relaxation is neglected since it is extremely slow when the hole is confined in the trion states.¹¹ The theory presented here can be extended straightforwardly to include the hole spin relaxation, the light-hole states, the hole mixing effect (which leads to the imperfection in the selection rules, for example, in InAs QDs), the multiexciton states, the inhomogeneous broadening of the trion states, and so on, but we expect no qualitative modification of the resonance features related to the electron spin coherence in the nonlinear optical spectra. For simplicity, we

shall consider only σ^+ -polarized optical fields (extension to other polarization configurations may provide some flexibility for experiments and is trivial in the theoretical part). Thus, the model is reduced to a Λ -type three-level system, consisting of the two electron spin states $|\pm\rangle$ and the trion state $|\tau\rangle$. The Λ -type three-level model, in spite of its simplicity, is the basis of a wealth of physical effects, including electromagnetically induced transparency,²⁷ lasing without inversion,²⁸ and stimulated Raman adiabatic passage,²⁹ and it has been successfully applied to study transient optical signals of doped QDs.^{3,30}

The dynamics of the system is described in the density matrix formalism with $\rho_{\alpha,\beta}$ as the density matrix elements between the states $|\alpha\rangle$ and $|\beta\rangle$. The optical excitation and relaxation are accounted for in the master equation as

$$\partial_t \rho_{\tau,\pm} = -i[\mathcal{E}_g \mp (\omega_0 + \epsilon)/2 - i\Gamma_2] \rho_{\tau,\pm} - iE(t) \rho_{\tau,\mp} + iE(t) \rho_{\mp,\pm} + iE(t) \rho_{\pm,\pm}, \quad (1a)$$

$$\partial_t \rho_{\tau,\tau} = -2\Gamma_1 \rho_{\tau,\tau} + 2\mathcal{J}[E^*(t) \rho_{\tau,+} + E^*(t) \rho_{\tau,-}], \quad (1b)$$

$$\partial_t \rho_{\pm,\pm} = -(\rho_{\mp,\pm} - \rho_{\pm,\mp})/T_1 + \Gamma_1 \rho_{\tau,\tau} - 2\mathcal{J}[E^*(t) \rho_{\tau,\pm}], \quad (1c)$$

$$\partial_t \rho_{\pm,\mp} = \Gamma_1 \rho_{\tau,\tau} - i[\pm(\omega_0 + \epsilon) - i/T_2] \rho_{\pm,\mp} + iE^*(t) \rho_{\tau,\mp} - iE(t) \rho_{\tau,\pm}, \quad (1d)$$

where \mathcal{E}_g is the energy gap and p_{\pm} is the equilibrium population of the spin states in the absence of the optical excitation; the optical field $E(t) = \sum_j E_j e^{-i\Omega_j t}$ contains different frequency components. The transition dipole moment is understood to be absorbed into the field quantities. In the rotating wave reference frame, the energy gap \mathcal{E}_g is set to be zero and the optical frequencies Ω_j are measured from the gap. The first term in the right-hand side of Eq. (1d) is the spin coherence generated by spontaneous emission,³⁰⁻³² which has been demonstrated in time-domain experiments with significant effects on spin beats.³ We will show that it produces extra resonances in the fifth-order DT spectra.

To calculate the nonlinear optical susceptibility, the master equation is obtained in the frequency domain (as given in the Appendix). With the spectrum of the optical field given by $E(\Omega) = \sum_j 2\pi E_j \delta(\Omega - \Omega_j)$, the density matrix can be expanded as

$$\rho_{\alpha,\beta}(\Omega) = \sum_{j,\dots,k;m,\dots,l} 2\pi E_j \cdots E_k E_m^* \cdots E_l^* \rho_{\alpha,\beta}^{(j,\dots,k;\bar{m},\dots,\bar{l})} \delta(\Omega - \Omega_{j,\dots,k;\bar{m},\dots,\bar{l}}), \quad (2)$$

where $\Omega_{j,\dots,k;\bar{m},\dots,\bar{l}} \equiv \Omega_j + \cdots + \Omega_k - (\Omega_m + \cdots + \Omega_l)$. The derivation of the density matrix component $\rho^{(j,\dots,k;\bar{m},\dots,\bar{l})}$ up to the fifth order is lengthy but straightforward. The final result is averaged with the inhomogeneous broadening distribution $g(\epsilon)$.

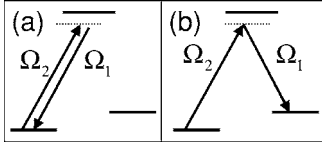


FIG. 2. Schematics of Raman processes generating (a) the spin population and (b) the off-diagonal spin coherence.

III. RESULTS AND DISCUSSIONS

The linear optical susceptibility is given by

$$\rho^{(j)} = \int \frac{g(\epsilon)}{\Omega_j - \mathcal{E}_g \pm (\omega_0 + \epsilon)/2 + i\Gamma_2} d\epsilon. \quad (3)$$

In fluctuation GaAs QDs, the exciton dephasing is much faster than the spin dephasing due to the inhomogeneous broadening ($\Gamma_2^{-1} \leq 0.1 \text{ ns} \ll T_2^* \sim 10 \text{ ns}$),³ so the resonance width in linear optical spectra is usually dominated by the trion state broadening, revealing little information about the spin decoherence.

In third-order optical response, the population and off-diagonal coherence of the electron spin are generated by the Raman processes,

$$\rho_{\pm,\pm} \xrightarrow{E_2} \rho_{\tau,\pm}^{(2)} \xrightarrow{E_1^*} \rho_{\pm,\pm}^{(2\bar{1})} \propto \left(\Omega_{2\bar{1}} + \frac{i}{T_1} \right)^{-1}, \quad (4a)$$

$$\rho_{\pm,\pm} \xrightarrow{E_2} \rho_{\tau,\pm}^{(2)} \xrightarrow{E_1^*} \rho_{\tau,\pm}^{(2\bar{1})} \propto \left[\Omega_{2\bar{1}} \pm (\omega_0 + \epsilon) + \frac{i}{T_2} \right]^{-1}, \quad (4b)$$

corresponding to the illustrations in Figs. 2(a) and 2(b), respectively. Another optical field with frequency Ω_1 brings the second-order spin coherence into the third-order optical coherence $\rho_{\tau,\pm}^{(2\bar{1})}$. The DT spectrum as a function of the pump frequency Ω_1 and the probe frequency Ω_2 is

$$S_{\text{DT}}(\Omega_2, \Omega_1) \propto -\Im[\rho_{\tau,+}^{(2\bar{1})} + \rho_{\tau,-}^{(2\bar{1})}], \quad (5)$$

which presents the ultranarrow resonances around $\Omega_{2\bar{1}} = 0$ and $\Omega_{2\bar{1}} = \pm \omega_0$, with resonance widths T_1^{-1} and T_2^{-1} , related to the spin population and off-diagonal coherence in Eqs. (4a) and (4b), respectively. Such resonances are shown in Fig. 3 (as dot black lines). Thus, the spin relaxation times T_1 and T_2 are measured, but when the inhomogeneous broadening is included, since usually $T_2 \gg T_2^*$, the Stokes and anti-Stokes Raman resonances at $\Omega_{2\bar{1}} = \pm \omega_0$ will be smeared to be a peak resembling the inhomogeneous broadening distribution as

$$\int \rho_{\tau,\mp}^{(2\bar{1})} g(\epsilon) d\epsilon \sim -i\pi g(\Omega_{2\bar{1}} \mp \omega_0). \quad (6)$$

The effect of the inhomogeneous broadening is clearly seen in Fig. 3 (solid red lines). So in usual cases, the third-order DT spectra measure the T_2^* instead of the T_2 . The resonance at degenerate pump and probe frequencies ($\Omega_{2\bar{1}} = 0$) is related to the spin population and is immune to the random distribution of the electron Zeeman energy. So the longitudinal spin relaxation time T_1 can be deduced from the third-order DT spectra, regardless of the inhomogeneous broadening.

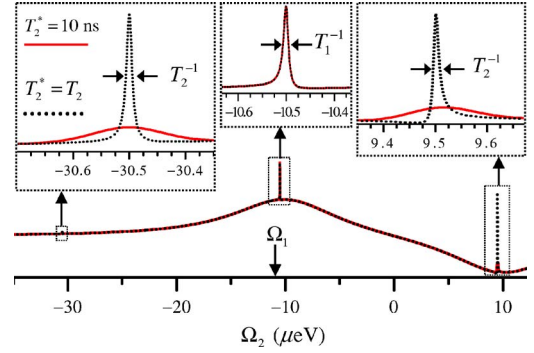


FIG. 3. (Color online) Third-order DT spectra of QDs doped with single electrons. The parameters are chosen such that the Zeeman energy $\omega_0 = 20 \mu\text{eV}$, the spin population $p_{\pm} = 0.5$, the pump frequency $\Omega_1 = \mathcal{E}_g - 10.5 \mu\text{eV}$, $\Gamma_1 = 5 \mu\text{eV}$ ($\Gamma_1^{-1} \approx 0.12 \text{ ns}$), $\Gamma_2 = 6 \mu\text{eV}$ ($\Gamma_2^{-1} \approx 0.1 \text{ ns}$), $T_1 = 100 \text{ ns}$, $T_2 = 100 \text{ ns}$, and $T_2^* = 10 \text{ ns}$ for the solid (red) lines and $T_2^* = T_2$ (no inhomogeneous broadening) for the dot (black) lines. The insets are enlarged plots, showing details of the resonances.

We note that the resonance features of the third-order susceptibility shown in Fig. 3 are consistent with the recent experimental data.¹⁸

To measure the transverse relaxation time excluding the inhomogeneous broadening effect, the fifth-order nonlinear optical response can be used. In the fifth-order optical response, the spin coherence in the fourth order of optical field has very rich resonance structures. For instance, a double resonance such as

$$\rho_{+,-}^{(432\bar{1})} \sim \frac{1}{\left[\Omega_{3\bar{1}} - (\omega_0 + \epsilon) + \frac{i}{T_2} \right] \left[\Omega_{432\bar{1}} - (\omega_0 + \epsilon) + \frac{i}{T_2} \right]} \quad (7)$$

arises from the excitation pathway

$$\rho_{-,-} \xrightarrow{E_3} \rho_{\tau,-}^{(3)} \xrightarrow{E_1^*} \rho_{+,-}^{(3\bar{1})} \xrightarrow{E_4} \rho_{\tau,-}^{(43\bar{1})} \xrightarrow{E_2^*} \rho_{+,-}^{(432\bar{1})}, \quad (8)$$

as depicted in Fig. 4(a). The double resonance will manifest itself in a two-dimensional DT spectrum as an ultranarrow peak at $\Omega_{3\bar{1}} = \Omega_{432\bar{1}} = \omega_0 + \epsilon$ with width of $\sim T_2^{-1}$. When the inhomogeneous broadening is included, the ultranarrow resonance will be smeared into a broadened peak along the direction $\Omega_{3\bar{1}} = \Omega_{432\bar{1}}$ with width of $\sim 1/T_2^*$, but in the perpen-

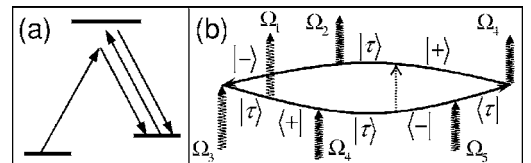


FIG. 4. (a) Schematics for a fourth-order optical process that generates spin coherence with a double resonance structure. (b) The Feynman diagram for the fifth-order optical response involving the spontaneous emission, in which the optical field and the vacuum field are represented by the wavy arrows and the dotted arrow, respectively.

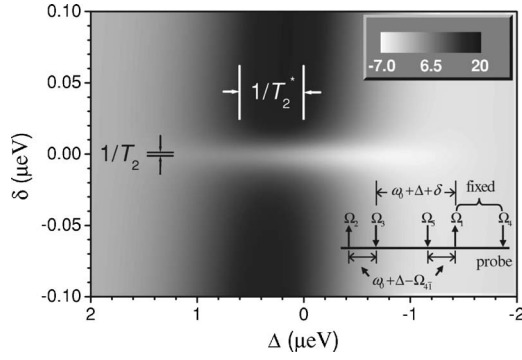


FIG. 5. Contour plot of the fifth-order DT spectrum of the QDs as a function of $\Delta \equiv \Omega_{432\bar{1}} - \omega_0$ and $\delta \equiv \Omega_{1\bar{3}} - \Omega_{432\bar{1}}$. The probe frequency is fixed to be $\Omega_4 = 22 \mu\text{eV}$, the pump frequency Ω_1 is fixed at $9 \mu\text{eV}$, and the other three pump frequencies are scanned with $\Omega_{532\bar{1}} = 0$ (which makes $\Omega_{1\bar{5}} = \Omega_{3\bar{2}} = \omega_0 + \Delta - \Omega_{4\bar{1}}$ and $\Omega_{1\bar{3}} = \Omega_{5\bar{2}} = \omega_0 + \Delta + \delta$, as indicated in the inset). The Zeeman energy $\omega_0 = 20 \mu\text{eV}$, the spin population $p_{\pm} = 0.5$, and the relaxation rates are such that $\Gamma_1 = 5 \mu\text{eV}$ ($\Gamma_1^{-1} \approx 0.12 \text{ ns}$), $\Gamma_2 = 6 \mu\text{eV}$ ($\Gamma_2^{-1} \approx 0.1 \text{ ns}$), $T_1 = 100 \text{ ns}$, $T_2 = 100 \text{ ns}$, and $T_2^* = 1 \text{ ns}$.

dicular direction (defined by $\Omega_{3\bar{1}} = -\Omega_{432\bar{1}}$), the peak width remains unchanged. So when $\Omega_{432\bar{1}}$ is fixed around ω_0 and $\Omega_{3\bar{1}}$ is scanned, or vice versa, the DT spectrum will present a sharp peak whose width measures the inverse transverse relaxation time T_2^{-1} . This peak has the character of hole burning: The first frequency difference acts just as a selection of QDs with Zeeman energy $\omega_0 + \epsilon = \Omega_{432\bar{1}}$ from the inhomogeneously broadened ensemble. The hole-burning resonance resulting from the excitation pathway in Eq. (8), however, emerges together with the resonance associated with the spin population $(\Omega_{4\bar{2}} + i/T_1)^{-1}$, as given in Eq. (4a). To avoid the complication of mixing two types of resonance structures, we would rather make use of another mechanism for spin coherence generation, namely, the spontaneous emission that connects the trion state to the two spin states through the vacuum field [related to the first term in the right-hand side of Eq. (1d)].^{3,30-32}

The generation of spin coherence in the fifth-order optical response involving the spontaneous emission can take a quantum pathway like

$$\rho_{-,-} \rightarrow \rho_{\tau,-}^{(3)} \xrightarrow{E_1^*} \rho_{+,-}^{(3\bar{1})} \xrightarrow{E_4} \rho_{\tau,-}^{(43\bar{1})} \xrightarrow{E_2^*} \rho_{\tau,\tau}^{(432\bar{1})} \xrightarrow{\Gamma_1} \rho_{-,+}^{(432\bar{1})}, \quad (9)$$

where the last step is the spontaneous emission. This optical process is illustrated by the Feynman diagram in Fig. 4(b). The spin coherence generated by the spontaneous emission and that by optical excitation can have opposite spin indices $[\rho_{+,-}^{(3\bar{1})} \rightarrow \rho_{-,+}^{(432\bar{1})}]$, which is impossible in quantum pathways without the spontaneous emission [as can be seen from Fig. 4(a)]. Thus, the double resonance becomes

$$\rho_{-,+}^{(432\bar{1})} \sim \frac{\Gamma_1 / (\Omega_{432\bar{1}} + i2\Gamma_1)}{\left[\Omega_{3\bar{1}} + (\omega_0 + \epsilon) + \frac{i}{T_2} \right] \left[\Omega_{432\bar{1}} - (\omega_0 + \epsilon) + \frac{i}{T_2} \right]}, \quad (10)$$

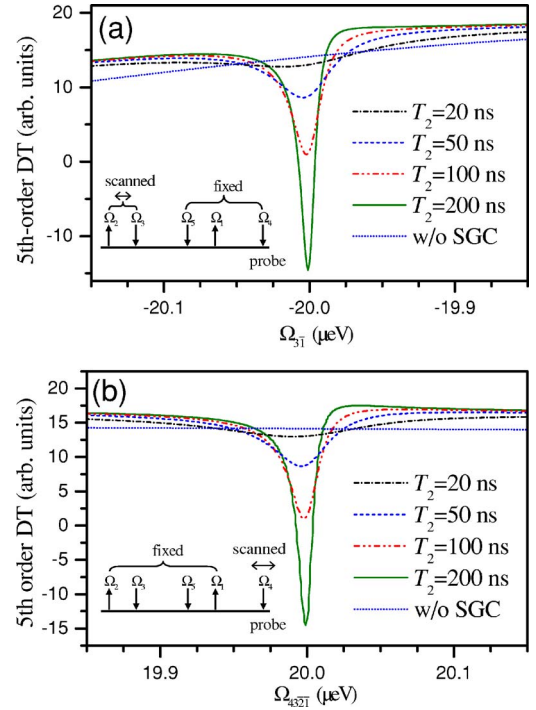


FIG. 6. (Color online) (a) The sectioned plot of Fig. 5 with $\Delta = 0$ (i.e., $\Omega_{432\bar{1}} = \omega_0$). (b) The fifth-order DT signal as a function of the probe frequency with pump frequencies fixed to be such that $\Omega_1 = 9 \mu\text{eV}$, $\Omega_5 = 2 \mu\text{eV}$, and $\Omega_{1\bar{3}} = \Omega_{5\bar{2}} = \omega_0 = 20 \mu\text{eV}$. In both figures, the transverse spin relaxation time $T_2 = 20, 50, 100,$ and 200 ns for the dash-dot (black), dash (blue), dash-dot-dot (red), and solid (green) lines from top to bottom, respectively, and the dot (blue) line is calculated with the spontaneously generated spin coherence artificially switched off (for $T_2 = 100 \text{ ns}$). The parameters are the same as in Fig. 5.

which is well separated from the spin population resonance. The spectrum is measured by fixing $\Omega_{432\bar{1}}$ to be the hole-burning frequency $\omega_0 + \Delta$ with $\Delta \lesssim 1/T_2^*$ and fine tuning $\Omega_{1\bar{3}}$ to be $\Omega_{432\bar{1}} + \delta$. As shown in the inset of Fig. 5, the optical frequencies can be configured such that Ω_4 and Ω_1 are fixed, Ω_3 are redshifted by $\omega_0 + \Delta + \delta$ from Ω_1 , and Ω_5 and Ω_2 are redshifted by $\omega_0 + \Delta - \Omega_{4\bar{1}}$ from Ω_1 and Ω_3 , respectively.

Thus, the fifth-order optical response $\rho_{\tau,\pm}^{(5432\bar{1})}$ oscillates at the probe frequency Ω_4 , which enables the signal to be measured in the DT setup instead of six-wave mixing ones. We note that the resonance due to the spin population $\sim (\Omega_{532\bar{1}} + i/T_1)^{-1}$ contributes only a constant background since $\Omega_{532\bar{1}} \equiv 0$ in the above frequency configuration. As shown in Fig. 5, which plots the fifth-order DT spectrum as a function of $\Delta \equiv \Omega_{432\bar{1}} - \omega_0$ and the fine tuning $\delta \equiv \Omega_{1\bar{3}} - \Omega_{432\bar{1}}$, a very narrow hole in the spectrum as a function of $\Omega_{3\bar{1}}$ is burnt around $\Omega_{432\bar{1}}$, with width given by T_2^{-1} . Along the direction $\Omega_{3\bar{1}} = -\Omega_{432\bar{1}}$ ($\delta = 0$), the resonance is extended by the inhomogeneous broadening as expected. Sectioned plots of the DT signal with fixed Δ are shown in Fig. 6(a) for various transverse relaxation time. The resonance width is given by the transverse relaxation rate, demonstrating unambiguously that the T_2 is measured by the hole-burning effect. The hole-burning resonance can also be detected by varying the probe

frequency with the pump frequencies fixed, as demonstrated in Fig. 6(b). The role of the spontaneous emission-generated spin coherence is verified by the absence of the ultranarrow resonance with artificial switch-off of the relevant term in Eq. (1d).

IV. CONCLUSIONS

The spin coherence can be generated and detected in nonlinear optical spectroscopy of quantum dots doped with single electrons, which is studied in this paper up to the fifth-order nonlinearity with a Λ -type three-level model. The electron spin coherence is generated by the optical field through Raman processes as well as by spontaneous emission of the trion. The spin population and off-diagonal coherence manifest themselves in third-order differential transmission spectra as ultranarrow resonances. The inhomogeneous broadening smears out the sharp Stokes and anti-Stokes peaks related to the off-diagonal spin coherence. Thus, the longitudinal spin relaxation time T_1 and the dephasing time T_2^* are measured by the third-order spectra. In the fifth-order optical response, the generation of the spin coherence by both second- and fourth-order optical processes leads to double resonance structures in two-dimensional DT spectra, which are smeared by the inhomogeneous broadening along one direction in the frequency space but presents ultranarrow hole-burning resonances along the perpendicular direction. So the transverse spin relaxation time T_2 is measured as the inverse width of the hole-burning peak. The

spontaneous emission-generated spin coherence^{3,30} is useful to produce hole-burning resonances well separated from the spin-population resonances in the fifth-order spectra. The frequencies of the optical field can be configured properly to enable the detection of the signal in the DT setup instead of the multiwave mixing ones. In practice, the pump and probe frequencies may be generated from a single continuous-wave laser source by, e.g., acousto-optical modulation.²⁶ Since the ultranarrow hole-burning peaks are rather insensitive to the global shift of the laser frequencies and variation of the hole-burning frequency, nonstabilized laser sources may be used to resolve the slow spin decoherence.²⁶ In the present research, the electron spin decoherence and the inhomogeneous broadening are parametrized with a few time scales (T_1 , T_2 , and T_2^*). The theoretical framework in this paper can be readily extended to study the effect of the spectral diffusion³³⁻³⁵ of the electron spin on the nonlinear optical spectroscopy. We expect that the leading-order effect of the spectral diffusion can also be eliminated in the fifth-order nonlinear optical susceptibility.

ACKNOWLEDGMENTS

This work was partially supported by the Hong Kong RGC Direct Grant 2060284 and by ARO/NSA-LPS.

APPENDIX: SOLUTION OF THE MASTER EQUATION

The master equation in Eq. (1) can be solved in the frequency domain by Fourier transformation to be

$$\rho_{\tau,\pm}(\Omega) = \int \frac{-E(\Omega - \omega)\rho_{\pm,\pm}(\omega) - E(\Omega - \omega)\rho_{\mp,\pm}(\omega) + E(\Omega - \omega)\rho_{\tau,\tau}(\omega) d\omega}{\Omega - \mathcal{E}_g \pm (\omega_0 + \epsilon)/2 + i\Gamma_2} \frac{d\omega}{2\pi}, \quad (\text{A1a})$$

$$\rho_{\tau,\tau}(\omega) = \sum_{\pm} \int \frac{+E^*(\Omega - \omega)\rho_{\tau,\pm}(\Omega) - E(\Omega + \omega)\rho_{\tau,\pm}^*(\Omega) d\Omega}{\omega + i2\Gamma_1} \frac{d\Omega}{2\pi}, \quad (\text{A1b})$$

$$\begin{aligned} \rho_{\pm,\pm}(\omega) &= p_{\pm} 2\pi \delta(\omega) - (\omega + i\Gamma_1 + ip_{\pm}/T_1) \int \frac{E^*(\Omega - \omega)\rho_{\tau,\pm}(\Omega) - E(\Omega + \omega)\rho_{\tau,\pm}^*(\Omega) d\Omega}{(\omega + i/T_1)(\omega + i2\Gamma_1)} \frac{d\Omega}{2\pi} \\ &+ (i\Gamma_1 - ip_{\pm}/T_1) \int \frac{E^*(\Omega - \omega)\rho_{\tau,\mp}(\Omega) - E(\Omega + \omega)\rho_{\tau,\mp}^*(\Omega) d\Omega}{(\omega + i/T_1)(\omega + i2\Gamma_1)} \frac{d\Omega}{2\pi}, \end{aligned} \quad (\text{A1c})$$

$$\rho_{+,-}(\omega) = \frac{i\Gamma_1 \rho_{\tau,\tau}(\omega)}{\omega - (\omega_0 + \epsilon) + i/T_2} + \int \frac{-E^*(\Omega - \omega)\rho_{\tau,-}(\Omega) + E(\Omega + \omega)\rho_{\tau,+}^*(\Omega) d\Omega}{\omega - (\omega_0 + \epsilon) + i/T_2} \frac{d\Omega}{2\pi}. \quad (\text{A1d})$$

- ¹*Semiconductor spintronics and quantum computation*, edited by D. D. Awschalom, D. Loss, and N. Samarth (Springer, New York, 2002).
- ²J. A. Gupta, D. D. Awschalom, A. L. Efros, and A. V. Rodina, *Phys. Rev. B* **66**, 125307 (2002).
- ³M. V. Gurudev Dutt, J. Cheng, B. Li, X. Xu, X. Li, P. R. Berman, D. G. Steel, A. S. Bracker, D. Gammon, S. E. Economou, R. B. Liu, and L. J. Sham, *Phys. Rev. Lett.* **94**, 227403 (2005).
- ⁴P. F. Braun, X. Marie, L. Lombez, B. Urbaszek, T. Amand, P. Renucci, V. K. Kalevich, K. V. Kavokin, O. Krebs, P. Voisin, and Y. Masumoto, *Phys. Rev. Lett.* **94**, 116601 (2005).
- ⁵A. Greilich, D. R. Yakovlev, A. Shabaev, A. L. Efros, I. A. Yugova, R. Oulton, V. Stavarache, D. Reuter, A. Wieck, and M. Bayer, *Science* **313**, 341 (2006).
- ⁶T. Fujisawa, D. G. Austing, Y. Tokura, Y. Hirayama, and S. Tarucha, *Nature (London)* **419**, 278 (2002).
- ⁷J. M. Elzerman, R. Hanson, L. H. Willems van Beveren, B. Witkamp, L. M. K. Vandersypen, and L. P. Kouwenhoven, *Nature (London)* **430**, 431 (2004).
- ⁸A. C. Johnson, J. R. Petta, J. M. Taylor, A. Yacoby, M. D. Lukin, C. M. Marcus, M. P. Hanson, and A. C. Gossard, *Nature (London)* **435**, 925 (2005).
- ⁹M. Kroutvar, Y. Ducommun, D. Heiss, M. Bichler, D. Schuh, D. Abstreiter, and J. J. Finley, *Nature (London)* **432**, 81 (2004).
- ¹⁰A. S. Bracker, E. A. Stinaff, D. Gammon, M. E. Ware, J. G. Tischler, A. Shabaev, A. L. Efros, D. Park, D. Gershoni, V. L. Korenev, and I. A. Merkulov, *Phys. Rev. Lett.* **94**, 047402 (2005).
- ¹¹M. Atattire, J. Dreiser, A. Högele, K. Karrai, and A. Imamoglu, *Science* **312**, 551 (2006).
- ¹²J. R. Petta, A. C. Johnson, J. M. Taylor, E. A. Laird, A. Yacoby, M. D. Lukin, C. M. Marcus, M. P. Hanson, and A. C. Gossard, *Science* **309**, 2180 (2005).
- ¹³F. H. L. Koppens, J. A. Folk, J. M. Elzerman, R. Hanson, L. H. W. van Beveren, I. T. Vink, H. P. Tranitz, W. Wegscheider, L. P. Kouwenhoven, and L. M. K. Vandersypen, *Science* **309**, 1346 (2005).
- ¹⁴F. H. L. Koppens, C. Buizert, K. J. Tielrooij, I. T. Vink, K. C. Nowack, T. Meunier, L. P. Kouwenhoven, and L. M. K. Vandersypen, *Nature (London)* **442**, 766 (2006).
- ¹⁵I. A. Merkulov, A. L. Efros, and M. Rosen, *Phys. Rev. B* **65**, 205309 (2002).
- ¹⁶Y. G. Semenov and K. W. Kim, *Phys. Rev. B* **67**, 073301 (2003).
- ¹⁷A. V. Khaetskii, D. Loss, and L. Glazman, *Phys. Rev. Lett.* **88**, 186802 (2002).
- ¹⁸J. Cheng, Y. W. Wu, X. D. Xu, D. Sun, D. G. Steel, A. S. Bracker, D. Gammon, W. Yao, and L. J. Sham, *Solid State Commun.* **140**, 381 (2006).
- ¹⁹A. M. Tyryshkin, S. A. Lyon, A. V. Astashkin, and A. M. Raitsimring, *Phys. Rev. B* **68**, 193207 (2003).
- ²⁰E. Abe, K. M. Itoh, J. Isoya, and S. Yamasaki, *Phys. Rev. B* **70**, 033204 (2004).
- ²¹E. Abe, J. Isoya, and K. M. Itoh, *J. Supercond.* **18**, 157 (2005).
- ²²P. Chen, C. Piermarocchi, L. J. Sham, D. Gammon, and D. G. Steel, *Phys. Rev. B* **69**, 075320 (2004).
- ²³D. G. Steel and J. T. Remillard, *Phys. Rev. A* **36**, 4330 (1987).
- ²⁴D. G. Steel and S. C. Rand, *Phys. Rev. Lett.* **55**, 2285 (1985).
- ²⁵N. M. Strickland, P. B. Sellin, Y. Sun, J. L. Carlsten, and R. L. Cone, *Phys. Rev. B* **62**, 1473 (2000).
- ²⁶S. Ohno, T. Ishii, T. Sonehara, A. Koreeda, and S. Saikan, *J. Lumin.* **107**, 298 (2004).
- ²⁷S. E. Harris, J. E. Field, and A. Imamoglu, *Phys. Rev. Lett.* **64**, 1107 (1990).
- ²⁸S. E. Harris, *Phys. Rev. Lett.* **62**, 1033 (1989).
- ²⁹K. Bergmann, H. Theuer, and B. W. Shore, *Rev. Mod. Phys.* **70**, 1003 (1998).
- ³⁰S. E. Economou, R. B. Liu, L. J. Sham, and D. G. Steel, *Phys. Rev. B* **71**, 195327 (2005).
- ³¹J. Javanainen, *Europhys. Lett.* **17**, 407 (1992).
- ³²A. Shabaev, A. L. Efros, D. Gammon, and I. A. Merkulov, *Phys. Rev. B* **68**, 201305(R) (2003).
- ³³P. W. Anderson, *J. Phys. Soc. Jpn.* **9**, 316 (1954).
- ³⁴R. Kubo, *J. Phys. Soc. Jpn.* **9**, 935 (1954).
- ³⁵P. R. Berman and R. G. Brewer, *Phys. Rev. A* **32**, 2784 (1985).